DEEP AUTOENCODING GAUSSIAN MIXTURE MODEL FOR UNSUPERVISED ANOMALY DETECTION

Anonymous authors
Paper under double-blind review

ABSTRACT

Unsupervised anomaly detection on multi- or high-dimensional data is of great importance in both fundamental machine learning research and industrial applications, for which density estimation lies at the core. Although previous approaches based on dimensionality reduction followed by density estimation have made fruitful progress, they mainly suffer from decoupled model learning with inconsistent optimization goals and incapability of preserving essential information in the low-dimensional space. In this paper, we present a Deep Autoencoding Gaussian Mixture Model (DAGMM) for unsupervised anomaly detection. Our model utilizes a deep autoencoder to generate a low-dimensional representation and reconstruction error for each input data point, which is further fed into a Gaussian Mixture Model (GMM). Instead of using decoupled two-stage training and the standard Expectation-Maximization (EM) algorithm, DAGMM jointly optimizes the parameters of the deep autoencoder and the mixture model simultaneously in an end-to-end fashion, leveraging a separate estimation network to facilitate the parameter learning of the mixture model. The joint optimization, which well balances autoencoding reconstruction, density estimation of latent representation, and regularization, helps the autoencoder escape from less attractive local optima and further reduce reconstruction errors, avoiding the need of pre-training. Experimental results on several public benchmark datasets show that, DAGMM significantly outperforms state-of-the-art anomaly detection techniques, and achieves up to 14% improvement based on the standard F_1 measure.

1 INTRODUCTION

Unsupervised anomaly detection is a fundamental problem in machine learning, with critical applications in many areas, such as cybersecurity (Tan et al. (2011)), complex system management (Liu et al. (2008)), medical care (Keller et al. (2012)), and so on. At the core of anomaly detection is density estimation: given a lot of input samples, anomalies are those ones residing in low probability density areas.

Although fruitful progress has been made in the last several years, conducting robust anomaly detection on multi- or high-dimensional data without human supervision remains a challenging task. Especially, when the dimensionality of input data becomes higher, it is more difficult to perform density estimation in the original feature space, as any input sample could be a rare event with low probability to observe (Chandola et al. (2009)). To address this issue caused by the curse of dimensionality, two-step approaches are widely adopted (Candès et al. (2011)), in which dimensionality reduction is first conducted, and then density estimation is performed in the latent low-dimensional space. However, these approaches could easily lead to suboptimal performance, because dimensionality reduction in the first step is unaware of the subsequent density estimation task, and the key information for anomaly detection could be removed in the first place. Therefore, it is desirable to combine the force of dimensionality reduction and density estimation, although a joint optimization accounting for these two components is usually computationally difficult. Several recent works (Zhai et al. (2016); Yang et al. (2017); Xie et al. (2016)) explored this direction by utilizing the strong modeling capacity of deep networks, but the resulting performance is limited either by a reduced low-dimensional space that is unable to preserve essential information of input samples, an over-simplified density estimation model without enough capacity, or a training strategy that does not fit density estimation tasks.

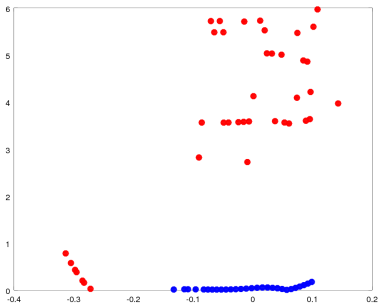

Figure 1: Low-dimensional representations for samples from a private cybersecurity dataset: (1) each sample denotes a network flow that originally has 20 dimensions, (2) red/blue points are abnormal/normal samples, (3) the horizontal axis denotes the reduced 1-dimensional space, and (4) the vertical axis denotes the reconstruction error induced by the 1-dimensional representation.

In this paper, we propose Deep Autoencoding Gaussian Mixture Model (DAGMM), a deep learning framework that addresses the aforementioned challenges in unsupervised anomaly detection from several aspects.

First, DAGMM preserves the key information of an input sample in a low-dimensional space that includes features from both the reduced dimensions discovered by dimensionality reduction and the induced reconstruction error. From the example shown in Figure 1, we can see that anomalies differ from normal samples in two aspects: (1) anomalies can be significantly deviated in the reduced dimensions where their features are correlated in a different way; and (2) anomalies are harder to reconstruct, compared with normal samples. Unlike existing methods that only involve one of the aspects (Zimek et al. (2012); Zhai et al. (2016)) with sub-optimal performance, DAGMM utilizes a sub-network called compression network to perform dimensionality reduction by an autoencoder, which prepares a low-dimensional representation for an input sample by concatenating reduced low-dimensional features from encoding and the reconstruction error from decoding.

Second, DAGMM leverages a Gaussian Mixture Model (GMM) over the learned low-dimensional space to deal with density estimation tasks for input data with complex structures, which are yet rather difficult for simple models used in existing works (Zhai et al. (2016)). While GMM has strong capability, it also introduces new challenges in model learning. As GMM is usually learned by alternating algorithms such as Expectation-Maximization (EM) (Huber (2011)), it is hard to perform joint optimization of dimensionality reduction and density estimation favoring GMM learning, which is often degenerated into a conventional two-step approach. To address this training challenge, DAGMM utilizes a sub-network called estimation network that takes the low-dimensional input from the compression network and outputs mixture membership prediction for each sample. With the predicted sample membership, we can directly estimate the parameters of GMM, facilitating the evaluation of the energy/likelihood of input samples. By simultaneously minimizing reconstruction error from compression network and sample energy from estimation network, we can jointly train a dimensionality reduction component that directly helps the targeted density estimation task.

Finally, DAGMM is friendly to end-to-end training. Usually, it is hard to learn deep autoencoders by end-to-end training, as they can be easily stuck in less attractive local optima, so pre-training is widely adopted (Vincent et al. (2010); Yang et al. (2017); Xie et al. (2016)). However, pre-training limits the potential to adjust the dimensionality reduction behavior because it is hard to make any significant change to a well-trained autoencoder via fine-tuning. Our empirical study demonstrates that, DAGMM is well-learned by the end-to-end training, as the regularization introduced by the estimation network greatly helps the autoencoder in the compression network escape from less attractive local optima.

Experiments on several public benchmark datasets demonstrate that, DAGMM has superior performance over state-of-the-art techniques, with up to 14% improvement of F1 score for anomaly detection. Moreover, we observe that the reconstruction error from the autoencoder in DAGMM by the end-to-end training is as low as the one made by its pre-trained counterpart, while the reconstruc-

tion error from an autoencoder without the regularization from the estimation network stays high. In addition, the end-to-end trained DAGMM significantly outperforms all the baseline methods that rely on pre-trained autoencoders.

2 RELATED WORK

Tremendous effort has been devoted to unsupervised anomaly detection (Chandola et al. (2009)), and the existing methods can be grouped into three categories.

Reconstruction based methods assume that anomalies are incompressible and thus cannot be effectively reconstructed from low-dimensional projections. Conventional methods in this category include Principal Component Analysis (PCA) (Jolliffe (1986)) with explicit linear projections, kernel PCA with implicit non-linear projections induced by specific kernels (Günter et al.), and Robust PCA (RPCA) (Huber (2011); Candès et al. (2011)) that makes PCA less sensitive to noise by enforcing sparse structures. In addition, multiple recent works propose to analyze the reconstruction error induced by deep autoencoders, and demonstrate promising results (Zhou & Paffenroth (2017); Zhai et al. (2016)). However, the performance of reconstruction based methods is limited by the fact that they only conduct anomaly analysis from a single aspect, that is, reconstruction error. Although the compression on anomalous samples could be different from the compression on normal samples and some of them do demonstrate unusually high reconstruction errors, a significant amount of anomalous samples could also lurk with a normal level of error, which usually happens when the underlying dimensionality reduction methods have high model complexity or the samples of interest are noisy with complex structures. Even in these cases, we still have the hope to detect such "lurking" anomalies, as they still reside in low-density areas in the reduced low-dimensional space. Unlike the existing reconstruction based methods, DAGMM considers the both aspects, and performs density estimation in a low-dimensional space derived from the reduced representation and the reconstruction error caused by the dimensionality reduction, for a comprehensive view.

Clustering analysis is another popular category of methods used for density estimation and anomaly detection, such as multivariate Gaussian Models, Gaussian Mixture Models, k-means, and so on (Barnett & Lewis (1984); Zimek et al. (2012); Kim & Scott (2011); Xiong et al. (2011)). Because of the curse of dimensionality, it is difficult to directly apply such methods to multi- or high- dimensional data. Traditional techniques adopt a two-step approach (Chandola et al. (2009)), where dimensionality reduction is conducted first, then clustering analysis is performed, and the two steps are separately learned. One of the drawbacks in the two-step approach is that dimensionality reduction is trained without the guidance from the subsequent clustering analysis, thus the key information for clustering analysis could be lost during dimensionality reduction. To address this issue, recent works propose deep autoencoder based methods in order to jointly learn dimensionality reduction and clustering components. However, the performance of the state-of-the-art methods is limited by over-simplified clustering models that are unable to handle clustering or density estimation tasks for data of complex structures, or the pre-trained dimensionality reduction component (*i.e.,* autoencoder) has little potential to accommodate further adjustment by the subsequent fine-tuning for anomaly detection. DAGMM explicitly addresses these issues by a sub-network called estimation network that evaluates sample density in the low-dimensional space produced by its compression network. By predicting sample mixture membership, we are able to estimate the parameters of GMM without EM-like alternating procedures. Moreover, DAGMM is friendly to end-to-end training so that we can unleash the full potential of adjusting dimensionality reduction components and jointly improve the quality of clustering analysis/density estimation.

In addition, one-class classification approaches are also widely used for anomaly detection. Under this framework, a discriminative boundary surrounding the normal instances is learned by algorithms, such as one-class SVM (Chen et al. (2001); Song et al. (2002); Williams et al. (2002)). When the number of dimensions grows higher, such techniques usually suffer from suboptimal performance due to the curse of dimensionality. Unlike these methods, DAGMM estimates data density in a jointly learned low-dimensional space for more robust anomaly detection.

3 DEEP AUTOENCODING GAUSSIAN MIXTURE MODEL

3.1 OVERVIEW

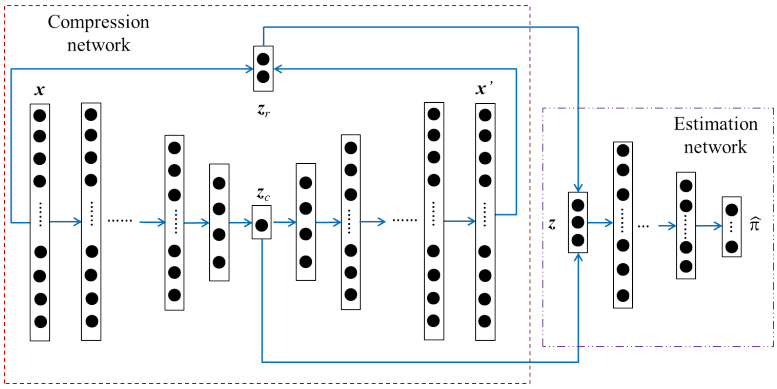

Figure 2: An overview on Deep Autoencoding Gaussian Mixture Model

Deep Autoencoding Gaussian Mixture Model (DAGMM) consists of two major components: a compression network and an estimation network. As shown in Figure 2, DAGMM works as follows: (1) the compression network performs dimensionality reduction for input samples by a deep autoencoder, prepares their low-dimensional representations from both the reduced space and the reconstruction error features, and feeds the representations to the subsequent estimation network; (2) the estimation network takes the feed, and predicts their likelihood/energy in the framework of Gaussian Mixture Model (GMM).

3.2 COMPRESSION NETWORK

The low-dimensional representations provided by the compression network contains two sources of features: (1) the reduced low-dimensional representations learned by a deep autoencoder; and (2) the features derived from reconstruction error. Given a sample $\mathbf{x}$, the compression network computes its low-dimensional representation $\mathbf{z}$ as follows.

$$\mathbf{z}_c = h(\mathbf{x}; \theta_e), \qquad \mathbf{x}' = g(\mathbf{z}_c; \theta_d), \tag{1}$$

$$\mathbf{z}_r = f(\mathbf{x}, \mathbf{x}'), \tag{2}$$

$$\mathbf{z} = [\mathbf{z}_c, \mathbf{z}_r], \tag{3}$$

where $\mathbf{z}_c$ is the reduced low-dimensional representation learned by the deep autoencoder, $\mathbf{z}_r$ includes the features derived from the reconstruction error, θ_e and θ_d are the parameters of the deep autoencoder, $\mathbf{x}'$ is the reconstructed counterpart of $\mathbf{x}$, $h(\cdot)$ denotes the encoding function, $g(\cdot)$ denotes the decoding function, and $f(\cdot)$ denotes the function of calculating reconstruction error features. In particular, $\mathbf{z}_r$ can be multi-dimensional, considering multiple distance metrics such as absolute Euclidean distance, relative Euclidean distance, cosine similarity, and so on. In the end, the compression network feeds $\mathbf{z}$ to the subsequent estimation network.

3.3 ESTIMATION NETWORK

Given the low-dimensional representations for input samples, the estimation network performs density estimation under the framework of GMM.

In the training phase with unknown mixture-component distribution ϕ, mixture means μ, and mixture covariance $\mathbf{\Sigma}$, the estimation network estimates the parameters of GMM and evaluates the likelihood/energy for samples without alternating procedures such as EM (Zimek et al. (2012)). The estimation network achieves this by utilizing a multi-layer neural network to predict the mixture membership for each sample. Given the low-dimensional representations $\mathbf{z}$ and an integer K as the number of mixture components, the estimation network makes membership prediction as follows.

$$\mathbf{p} = MLN(\mathbf{z}; \theta_m), \qquad \hat{\gamma} = \text{softmax}(\mathbf{p}), \tag{4}$$

where $\hat{\gamma}$ is a K-dimensional vector for the soft mixture-component membership prediction, and $\mathbf{p}$ is the output of a multi-layer network parameterized by θ_m. Given a batch of N samples and their membership prediction, $\forall 1 \leq k \leq K$, we can further estimate the parameters in GMM as follows.

$$\hat{\phi}_k = \sum_{i=1}^{N} \frac{\hat{\gamma}_{ik}}{N}, \qquad \hat{\mu}_k = \frac{\sum_{i=1}^{N} \hat{\gamma}_{ik} \mathbf{z}_i}{\sum_{i=1}^{N} \hat{\gamma}_{ik}}, \qquad \hat{\mathbf{\Sigma}}_k = \frac{\sum_{i=1}^{N} \hat{\gamma}_{ik} (\mathbf{z}_i - \hat{\mu}_k)(\mathbf{z}_i - \hat{\mu}_k)^T}{\sum_{i=1}^{N} \hat{\gamma}_{ik}}. \tag{5}$$

where $\hat{\gamma}_i$ is the membership prediction for the low-dimensional representation $\mathbf{z}_i$, and $\hat{\phi}_k$, $\hat{\mu}_k$, $\hat{\mathbf{\Sigma}}_k$ are mixture probability, mean, covariance for component k in GMM, respectively.

With the estimated parameters, sample energy can be further inferred by

$$E(\mathbf{z}) = -\log\left(\sum_{k=1}^{K} \hat{\phi}_k \frac{\exp\big(-\frac{1}{2}(\mathbf{z} - \hat{\mu}_k)^T \hat{\mathbf{\Sigma}}_k^{-1} (\mathbf{z} - \hat{\mu}_k)\big)}{\sqrt{|2\pi \hat{\mathbf{\Sigma}}_k|}}\right). \tag{6}$$

where $|\cdot|$ denotes the determinant of a matrix.

In addition, during the testing phase with the learned GMM parameters, it is straightforward to estimate sample energy, and predict samples of high energy as anomalies by a pre-chosen threshold.

3.4 Objective function

Given a dataset of N samples, the objective function that guides DAGMM training is constructed as follows.

$$J(\theta_e, \theta_d, \theta_m) = \frac{1}{N} \sum_{i=1}^{N} L(\mathbf{x}_i, \mathbf{x}'_i) + \frac{\lambda_1}{N} \sum_{i=1}^{N} E(\mathbf{z}_i) + \lambda_2 P(\hat{\mathbf{\Sigma}}). \tag{7}$$

This objective function includes three components.

- $L(\mathbf{x}_i, \mathbf{x}'_i)$ is the loss function that characterizes the reconstruction error caused by the deep autoencoder in the compression network. Intuitively, if the compression network could make the reconstruction error low, the low-dimensional representation could better preserve the key information of input samples. Therefore, a compression network of lower reconstruction error is always desired. In practice, L_2-norm usually gives desirable results, as $L(\mathbf{x}_i, \mathbf{x}'_i) = \|\mathbf{x}_i - \mathbf{x}'_i\|_2^2$.
- $E(\mathbf{z}_i)$ models the probabilities that we could observe the input samples. By minimizing the sample energy, we look for the best combination of compression and estimation networks that maximize the likelihood to observe input samples.
- DAGMM also has the singularity problem as in GMM: trivial solutions are triggered when the diagonal entries in covariance matrices degenerate to 0. To avoid this issue, we penalize small values on the diagonal entries by $P(\hat{\mathbf{\Sigma}}) = \sum_{k=1}^{K} \sum_{j=1}^{d} \frac{1}{\hat{\mathbf{\Sigma}}_{kjj}}$, where d is the number of dimensions in the low-dimensional representations provided by the compression network.
- λ_1 and λ_2 are the meta parameters in DAGMM. In practice, $\lambda_1 = 0.1$ and $\lambda_2 = 0.005$ usually render desirable results.

3.5 Training Strategy

Unlike existing deep autoencoder based methods (Yang et al. (2017); Xie et al. (2016)) that rely on pre-training, DAGMM employs end-to-end training. First, in our study, we find that pre-trained compression networks suffer from limited anomaly detection performance, as it is difficult to make significant changes in the well-trained deep autoencoder to favor the subsequent density estimation tasks. Second, we also find that the compression network and estimation network could mutually boost each others' performance. On one hand, with the regularization introduced by the estimation network, the deep autoencoder in the compression network learned by end-to-end training can reduce reconstruction error as low as the error from its pre-trained counterpart, which meanwhile cannot be achieved by simply performing end-to-end training with the deep autoencoder alone. On the other

hand, with the well-learned low-dimensional representations from the compression network, the estimation network is able to make meaningful density estimations.

In Section 4.5, we employ an example from a public benchmark dataset to discuss the choice between pre-training and end-to-end training in DAGMM.

4 EXPERIMENTAL RESULTS

In this section, we use public benchmark datasets to demonstrate the effectiveness of DAGMM in unsupervised anomaly detection.

4.1 DATASET

	# Dimensions	# Instances	Anomaly ratio (ρ)
KDDCUP	120	494,021	0.2
Thyroid	6	3,772	0.025
Arrhythmia	274	452	0.15

Table 1: Statistics of the public benchmark datasets

In this study, we employ three benchmark datasets: KDDCUP, Thyroid, and Arrhythmia.

- **KDDCUP**. The KDDCUP99 10 percent dataset from the UCI repository (Lichman (2013)) originally contains samples of 41 dimensions, where 34 of them are continuous and 7 are categorical. For categorical features, we further use one-hot representation to encode them, and eventually we obtain a dataset of 120 dimensions. As 20% of data samples are labeled as "normal" and the rest are labeled as attacks, "normal" samples are in a minority group; therefore, "normal" ones are treated as anomalies in this task.
- **Thyroid**. The Thyroid (Lichman (2013)) dataset is obtained from the ODDS repository [1]. There are 3 classes in the original dataset. In this task, the hyperfunction class is treated as anomaly class and the other two classes are treated as normal class, because hyperfunction is a clear minority class.
- **Arrhythmia**. The Arrhythmia (Lichman (2013)) dataset is also obtained from the ODDS repository. The smallest classes, including 3, 4, 5, 7, 8, 9, 14, and 15, are combined to form the anomaly class, and the rest of the classes are combined to form the normal class.

More detailed information about the datasets is shown in Table 1.

Following the setting in (Zhai et al. (2016)), in each run, we take 50% of data by random sampling for training with the rest 50% reserved for testing, and only data samples from the normal class are used for training models.

4.2 BASELINE METHODS

We consider both traditional and state-of-the-art deep learning methods as baselines.

- OC-SVM. One-class support vector machine (Chen et al. (2001)) is a popular kernel-based method used in anomaly detection. In the experiment, we employ the widely adopted radial basis function (RBF) kernel in all the tasks.
- DSEBM-e. Deep structured energy based model (DSEBM) (Zhai et al. (2016)) is a state-of-the-art deep learning method for unsupervised anomaly detection. In DSEBM-e, sample energy is leveraged as the criterion to detect anomalies.
- DSEBM-r. DSEBM-e and DSEBM-r (Zhai et al. (2016)) share the same core technique, but reconstruction error is used as the criterion in DSEBM-r for anomaly detection.

[1] http://odds.cs.stonybrook.edu/

- DCN. Deep clustering network (DCN) (Yang et al. (2017)) is a state-of-the-art clustering algorithm that regulates autoencoder performance by k-means. We adapt this technique to anomaly detection tasks. In particular, the distance between a sample and its cluster center is taken as the criterion for anomaly detection: samples that are farther from their cluster centers are more likely to be anomalies.

Moreover, we include the following DAGMM variants as baselines to demonstrate the importance of individual components in DAGMM.

- GMM-EN. In this variant, we remove the reconstruction error component from the objective function of DAGMM. In other words, the estimation network in DAGMM performs membership estimation without the constraints from the compression network. With the learned membership estimation, we infer sample energy by Equation (5) and (6) under the GMM framework. Sample energy is used as the criterion for anomaly detection.
- PAE. We obtain this variant by removing the energy function from the objective function of DAGMM, and this DAGMM variant is equivalent to a deep autoenoder. To ensure the compression network is well trained, we adopt the pre-training strategy (Vincent et al. (2010)). Sample reconstruction error is the criterion for anomaly detection.
- E2E-AE. This variant shares the same setting with PAE, but the deep autoencoder is learned by end-to-end training. Sample reconstruction error is the criterion for anomaly detection
- PAE-GMM. This variant adopts a two-step approach. At step one, we learn the compression network by pre-training deep autoencoder. At step two, we use the output from the compression network to train the estimation network. The training procedures in the two steps are separated. Sample energy is used as the criterion for anomaly detection.
- DAGMM-p. This variant is a compromise between DAGMM and PAE-GMM: we first train the compression network by pre-training, and then fine-tune DAGMM by end-to-end training. Sample energy is the criterion for anomaly detection.

4.3 DAGMM Configuration

In all the experiment, we consider two reconstruction features from the compression network: relative Euclidean distance and cosine similarity. Given a sample $\mathbf{x}$ and its reconstructed counterpart $\mathbf{x}'$, their relative Euclidean distance is defined as $\frac{\|\mathbf{x}-\mathbf{x}'\|_2}{\|\mathbf{x}\|_2}$, and the cosine similarity is derived by $\frac{\mathbf{x}\cdot\mathbf{x}'}{\|\mathbf{x}\|_2\|\mathbf{x}'\|_2}$.

The network structures of DAGMM used on individual datasets are summarized as follows.

- KDDCUP. For this dataset, its compression network provides 3 dimensional input to the estimation network, where one is the reduced dimension and the other two are from the reconstruction error. The estimation network considers a GMM with 4 mixture components for the best performance. In particular, the compression network runs with FC(120, 60, $\tanh$)-FC(60, 30, $\tanh$)-FC(30, 10, $\tanh$)-FC(10, 1, none)-FC(1, 10, $\tanh$)-FC(10, 30, $\tanh$)-FC(30, 60, $\tanh$)-FC(60, 120, none), and the estimation network performs with FC(3, 10, $\tanh$)-Drop(0.5)-FC(10, 4, softmax).
- Thyroid. The compression network for this dataset also provides 3 dimensional input to the estimation network, and the estimation network employs 2 mixture components for the best performance. In particular, the compression network runs with FC(6, 12, $\tanh$)-FC(12, 4, $\tanh$)-FC(4, 1, none)-FC(1, 4, $\tanh$)-FC(4, 12, $\tanh$)-FC(12, 6, none), and the estimation network performs with FC(3, 10, $\tanh$)-Drop(0.5)-FC(10, 2, softmax).
- Arrhythmia. The compression network for this dataset provides 4 dimensional input, where two of them are the reduced dimensions, and the estimation network adopts a setting of 2 mixture components for the best performance. In particular, the compression network runs with FC(274, 10, $\tanh$)-FC(10, 2, none)-FC(2, 10, $\tanh$)-FC(10, 274, none), and the estimation network performs with FC(4, 10, $\tanh$)-Drop(0.5)-FC(10, 2, softmax).

where FC(a, b, f) means a fully-connected layer with a input neurons and b output neurons activated by function f (none means no activation function is used), and Drop(p) denotes a dropout layer with keep probability p during training.

All the DAGMM instances are implemented by tensorflow (Abadi et al. (2016)) and trained by Adam (Kingma & Ba (2015)) algorithm with learning rate 0.0001. For KDDCUP, Thyroid, and Arrhythmia, the number of training epochs are 200, 20000, and 10000, respectively. For the sizes of mini-batches, they are set as 1024, 1024, and 128, respectively. Moreover, in all the DAGMM instances, we set λ_1 as 0.1 and λ_2 as 0.005.

For the baseline methods, we conduct exhaustive search to find the optimal meta parameters for them in order to achieve the best performance. We detail their exact configuration in Appendix A.

4.4 ACCURACY

Metric. We consider average precision, recall, and F_1 score as intuitive ways to compare anomaly detection performance. In particular, based on the anomaly ratio suggested in Table 1, we select the threshold to identify anomalous samples. For example, when DAGMM performs on KDDCUP, the top 20% samples of the highest energy will be marked as anomalies. We take anomaly class as positive, and define precision, recall, and F_1 score accordingly.

Method	KDDCUP			Thyroid			Arrhythmia		
	Precision	Recall	F_1	Precision	Recall	F_1	Precision	Recall	F_1
OC-SVM	0.7457	0.8523	0.7954	0.3639	0.4239	0.3887	**0.5397**	0.4082	0.4581
DSEBM-r	0.8521	0.6472	0.7328	0.0404	0.0403	0.0403	0.1515	0.1513	0.1510
DSEBM-e	0.8619	0.6446	0.7399	0.1319	0.1319	0.1319	0.4667	0.4565	0.4601
DCN	0.7696	0.7829	0.7762	0.3319	0.3196	0.3251	0.3758	0.3907	0.3815
GMM-EN	0.1932	0.1967	0.1949	0.0213	0.0227	0.0220	0.3000	0.2792	0.2886
PAE	0.7276	0.7397	0.7336	0.1894	0.2062	0.1971	0.4393	0.4437	0.4403
E2E-AE	0.0024	0.0025	0.0024	0.1064	0.1316	0.1176	0.4667	0.4538	0.4591
PAE-GMM	0.7251	0.7384	0.7317	0.4532	**0.4881**	0.4688	0.4575	0.4823	0.4684
DAGMM-p	0.7579	0.7710	0.7644	0.4723	0.4725	0.4713	0.4909	0.4679	0.4787
DAGMM	**0.9297**	**0.9442**	**0.9369**	**0.4766**	0.4834	**0.4782**	0.4909	**0.5078**	**0.4983**

Table 2: Average precision, recall, and F_1 from DAGMM and the baseline methods. For each metric, the best result is shown in bold.

Table 2 reports the average precision, recall, and F_1 score after 20 runs for DAGMM and its baselines. In general, DAGMM demonstrates superior performance over the baseline methods at almost all the ends. Especially on KDDCUP dataset, DAGMM achieves 14% improvement at F_1 score, compared with the closest baseline. For OC-SVM, the curse of dimensionality could be the main reason that limits its performance. For DSEBM, it performs reasonably well on Arrhythmia, but it is unable to handle data of more complex structures, such as KDDCUP and Thyroid. For DCN, PAE-GMM, and DAGMM-p, their performance could be limited by the pre-trained deep autoencoders. When a deep autoencoder is well-trained, it is hard to make any significant change on the reduced dimensions and favor the subsequent density estimation tasks. For GMM-EN, without the reconstruction constraints, it seems difficult to perform reasonable density estimation. In terms of PAE, the single view of reconstruction error may not be sufficient for anomaly detection tasks. For E2E-AE, we observe that it is unable to reduce reconstruction error as low as PAE and DAGMM do on KDDCUP and Thyroid. As the key information of data could be lost during dimensionality reduction, E2E-AE suffers poor performance on KDDCUP and Thyroid.

In sum, the DAGMM learned by end-to-end training achieves the best accuracy on the public benchmark datasets, and provides a promising alternative for unsupervised anomaly detection tasks.

4.5 VISUALIZATION ON THE LEARNED LOW-DIMENSIONAL REPRESENTATION

In this section, we use an example to demonstrate the advantage of DAGMM learned by end-to-end training, compared with the baselines that rely on pre-trained deep autoencoders.

Figure 3 shows the low-dimensional representation learned by DAGMM, PAE, DAGMM-p, and DCN, from one of the experiment runs on the KDDCUP dataset. First, we can clearly see from Figure 3a that DAGMM is able to well separate anomalous samples from normal samples in the

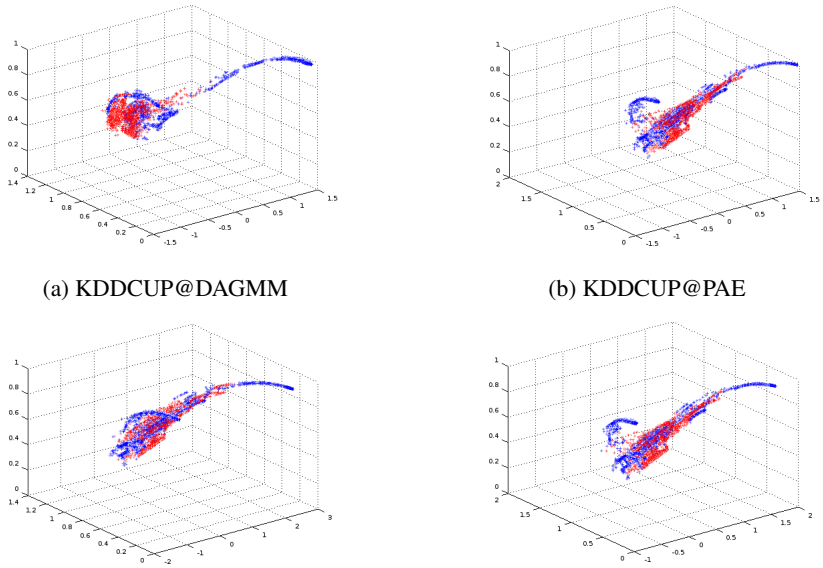

(a) KDDCUP@DAGMM

(b) KDDCUP@PAE

(c) KDDCUP@DAGMM-p

(d) KDDCUP@DCN

Figure 3: KDDCUP samples in the learned 3-dimensional space by DAGMM, PAE, DAGMM-p, and DCN, where red points are samples from anomaly class and blue ones are samples from normal class

learned low-dimensional space, while anomalies overlap with normal samples in the low-dimensional space learned by PAE, DAGMM-p, or DCN. Second, Even if DAGMM-p and DCN take effort to fine-tune the pre-trained deep autoencoder by its estimation network or k-means regularization, one could barely see significant change among Figure 3b, Figure 3c, and Figure 3d, where many anomalous samples are still mixed with normal samples. Indeed, when a deep autoencoder is pre-trained, it tends to be stuck in a good local optima for the purpose of reconstruction only, but it could be suboptimal for the subsequent density estimation tasks. In addition, in our study, we find that the reconstruction error in a trained DAGMM is as low as the error received from a pre-trained deep autoencoder (*e.g.,* around 0.26 in terms of per-sample reconstruction error for KDDCUP). Meanwhile, we also observe that it is difficult to reduce the reconstruction error for a deep autoencoder of the identical structure by end-to-end training (*e.g.,* around 1.13 in terms of per-sample reconstruction error for KDDCUP). In other words, the compression network and estimation network mutually boost each others' performance during end-to-end training: the regularization introduced by the estimation network helps the deep autoencoder escape from less attractive local optima for better compression, while the compression network feeds meaningful low-dimensional representations to estimation network for robust density estimation.

In summary, our experimental results show that DAGMM suggests a promising direction for density estimation and anomaly detection, where one can combine the forces of dimensionality reduction and density estimation by end-to-end training.

5 Conclusion

In this paper, we propose the Deep Autoencoding Gaussian Mixture Model (DAGMM) for unsupervised anomaly detection. DAGMM consists of two major components: compression network and estimation network, where the compression network projects samples into a low-dimensional space that preserves the key information for anomaly detection, and the estimation network evaluates sample energy in the low-dimensional space under the framework of Gaussian Mixture Modeling. DAGMM is friendly to end-to-end training: (1) the estimation network predicts sample mixture membership so that the parameters in GMM can be estimated without alternating procedures; and (2) the regularization introduced by the estimation network helps the compression network escape from less attractive local optima and achieve low reconstruction error by end-to-end training. Compared with

the pre-training strategy, the end-to-end training could be more beneficial for density estimation tasks, as we can have more freedom to adjust dimensionality reduction processes to favor the subsequent density estimation tasks. In the experimental study, DAGMM demonstrates superior performance over state-of-the-art techniques on public benchmark datasets with up to 14% improvement on the standard F_1 score, and suggests a promising direction for unsupervised anomaly detection on multi- or high-dimensional data.

REFERENCES

Martín Abadi, Paul Barham, Jianmin Chen, Zhifeng Chen, Andy Davis, Jeffrey Dean, Matthieu Devin, Sanjay Ghemawat, Geoffrey Irving, Michael Isard, et al. Tensorflow: A system for large-scale machine learning. In *OSDI*, volume 16, pp. 265–283, 2016.

V. Barnett and T. Lewis. *Outliers in statistical data*. Wiley, 1984.

Emmanuel J. Candès, Xiaodong Li, Yi Ma, and John Wright. Robust principal component analysis? *J. ACM*, 58(3):11:1–11:37, 2011. ISSN 0004-5411.

Varun Chandola, Arindam Banerjee, and Vipin Kumar. Anomaly detection: A survey. *ACM Comput. Surv*, 41:15:1–15:58, 2009.

Yunqiang Chen, Xiang Sean Zhou, and Thomas S Huang. One-class svm for learning in image retrieval. In *International Conference on Image Processing*, volume 1, pp. 34–37, 2001.

Simon Günter, Nicol N. Schraudolph, and S. V. N. Vishwanathan. Fast Iterative Kernel Principal Component Analysis. *jmlr*, 8:1893–1918.

Peter J Huber. Robust statistics. In *International Encyclopedia of Statistical Science*, pp. 1248–1251. Springer, 2011.

I. T. Jolliffe. Principal component analysis. In *Principal Component Analysis*. Springer Verlag, New York, 1986.

Fabian Keller, Emmanuel Muller, and Klemens Bohm. Hics: High contrast subspaces for density-based outlier ranking. In *International Conference on Data Engineering*, pp. 1037–1048. IEEE, 2012.

JooSeuk Kim and Clayton D. Scott. Robust kernel density estimation. *CoRR*, abs/1107.3133, 2011.

Diederik Kingma and Jimmy Ba. Adam: A method for stochastic optimization. In *International Conference for Learning Representations*, 2015.

M. Lichman. UCI machine learning repository, 2013. URL `http://archive.ics.uci.edu/ml`.

Fei Tony Liu, Kai Ming Ting, and Zhi-Hua Zhou. Isolation forest. In *International Conference on Data Mining*, pp. 413–422. IEEE, 2008.

Q. Song, W. J. Hu, and W. F. Xie. Robust support vector machine with bullet hole image classification. *IEEE Trans. Systems, Man and Cybernetics*, 32:440–448, 2002.

Swee Chuan Tan, Kai Ming Ting, and Tony Fei Liu. Fast anomaly detection for streaming data. In *IJCAI Proceedings-International Joint Conference on Artificial Intelligence*, volume 22, pp. 1511, 2011.

Pascal Vincent, Hugo Larochelle, Isabelle Lajoie, Yoshua Bengio, and Pierre-Antoine Manzagol. Stacked denoising autoencoders: Learning useful representations in a deep network with a local denoising criterion. *Journal of Machine Learning Research*, 11(Dec):3371–3408, 2010.

Graham Williams, Rohan Baxter, Hongxing He, and Simon Hawkins. A comparative study of RNN for outlier detection in data mining. In *Proceedings of ICDM02*, pp. 709–712, 2002.

Junyuan Xie, Ross Girshick, and Ali Farhadi. Unsupervised deep embedding for clustering analysis. In *International Conference on Machine Learning*, pp. 478–487, 2016.

Liang Xiong, Barnabás Póczos, and Jeff G. Schneider. Group anomaly detection using flexible genre models. In *Advances in Neural Information Processing Systems*, pp. 1071–1079, 2011.

Bo Yang, Xiao Fu, Nicholas D Sidiropoulos, and Mingyi Hong. Towards k-means-friendly spaces: Simultaneous deep learning and clustering. In *International Conference on Machine Learning*, 2017.

Shuangfei Zhai, Yu Cheng, Weining Lu, and Zhongfei Zhang. Deep structured energy based models for anomaly detection. In *International Conference on Machine Learning*, pp. 1100–1109, 2016.

Chong Zhou and Randy C. Paffenroth. Anomaly detection with robust deep autoencoders. In *Proceedings of the 23rd ACM SIGKDD International Conference on Knowledge Discovery and Data Mining*, pp. 665–674, 2017.

Arthur Zimek, Erich Schubert, and Hans-Peter Kriegel. A survey on unsupervised outlier detection in high-dimensional numerical data. *Statistical Analysis and Data Mining*, 5:363–387, 2012.

A BASELINE CONFIGURATION

OC-SVM. Unlike other baselines that only need decision thresholds in the testing phase, OC-SVM needs parameter ν be set in the training phase. Although ν intuitively means anomaly ratio in training data, it is non-trivial to set a reasonable ν in the case where training data are all normal samples and anomaly ratio in the testing phase could be arbitrary. In this study, we simply perform exhaustive search to find the optimal ν that renders the highest F_1 score on individual datasets. In particular, ν is set to be 0.1, 0.02, and 0.04 for KDDCUP, Thyroid, and Arrhythmia, respectively.

DSEBM. We use the network structure for the encoding in DAGMM as guidelines to set up DSEBM instances. For KDDCUP, it is configured as FC(120, 60, softplus)-FC(60, 30, softplus)-FC(30, 10, softplus)-FC(10, 1, softplus). For Thyroid, it is FC(6, 12, softplus)-FC(12, 4, softplus)-FC(4, 1, softplus). For Arrhythmia, it is FC(274, 10, softplus)-FC(10, 2, softplus). Moreover, for KDDCUP, Thyroid, and Arrhythmia, the numbers of epochs are 200, 20000, and 10000, respectively, and the sizes of mini-batches are 1024, 1024, and 128, respectively.

DCN. We use the network configuration for the autoencoder in DAGMM as guidelines to set up autoencoders in DCN. For KDDCUP, the structure is FC(120, 60, $\tanh$)-FC(60, 30, $\tanh$)-FC(30, 10, $\tanh$)-FC(10, 1, none)-FC(1, 10, $\tanh$)-FC(10, 30, $\tanh$)-FC(30, 60, $\tanh$)-FC(60, 120, none). For Thyroid, it is FC(6, 12, $\tanh$)-FC(12, 4, $\tanh$)-FC(4, 1, none)-FC(1, 4, $\tanh$)-FC(4, 12, $\tanh$)-FC(12, 6, none). For Arrhythmia, it is FC(274, 10, $\tanh$)-FC(10, 2, none)-FC(2, 10, $\tanh$)-FC(10, 274, none). Moreover, for KDDCUP, Thyroid, and Arrhythmia, the numbers of epochs for per-layer pre-training are 200, 20000, and 10000, respectively, the numbers of epochs for fine tuning are 200, 20000, and 10000, respectively, and the sizes of mini-batches in all the training phases are 1024, 1024, and 128, respectively.

GMM-EN. GMM-EN also borrows the wisdom from the network configurations in DAGMM. For KDD, it is FC(120, 60, $\tanh$)-FC(60, 30, $\tanh$)-FC(30, 10, $\tanh$)-FC(10, 1, none)-FC(1, 10, $\tanh$)-Drop(0.5)-FC(10, 4, softmax). For Thyroid, it is FC(6, 12, $\tanh$)-FC(12, 4, $\tanh$)-FC(4, 1, none)-FC(1, 10, $\tanh$)-Drop(0.5)-FC(10, 2, softmax). For Arrhythmia, it is FC(274, 10, $\tanh$)-FC(10, 2, none)-FC(2, 10, $\tanh$)-Drop(0.5)-FC(10, 2, softmax). For KDDCUP, Thyroid, and Arrhythmia, the numbers of epochs for training are 200, 20000, and 10000, respectively, and the sizes of mini-batches are 1024, 1024, and 128, respectively.

PAE. PAE share identical network structures with the autoencoder in DAGMM. For KDDCUP, Thyroid, and Arrhythmia, the numbers of epochs for per-layer pre-training are 200, 20000, and 10000, respectively, the numbers of epochs for fine tuning are 200, 20000, and 10000, respectively, and the sizes of mini-batches in all the training phases are 1024, 1024, and 128, respectively.

E2E-AE. E2E-AE share identical network structures with the autoencoder in DAGMM. For KDD-CUP, Thyroid, and Arrhythmia, the numbers of epochs for end-to-end training are 200, 20000, and 10000, respectively, and the sizes of mini-batches are 1024, 1024, and 128, respectively.

PAE-GMM. PAE-GMM and DAGMM share identical network configurations, but they differ in training strategies. For KDDCUP, Thyroid, and Arrhythmia, the numbers of epochs for per-layer pre-training are 200, 20000, and 10000, respectively, the numbers of epochs for fine tuning or GMM training are 200, 20000, and 10000, respectively, and the sizes of mini-batches in all the training phases are 1024, 1024, and 128, respectively.

DAGMM-p. DAGMM-p and DAGMM share identical network configurations, but they are only different in training strategies: DAGMM adopts the strategy of end-to-end training, while DAGMM-p relies on pre-training to compression network and then joint fine-tuning. For KDDCUP, Thyroid, and Arrhythmia, the numbers of epochs for per-layer pre-training are 200, 20000, and 10000, respectively, the numbers of epochs for fine tuning are 200, 20000, and 10000, respectively, and the sizes of mini-batches in all the training phases are 1024, 1024, and 128, respectively.